ISSN 1330-3651 (Print), ISSN 1848-6339 (Online)
https://doi.org/10.17559/TV-20240616001778
Original scientific paper

Enhancing Efficiency and Stability in a Multigenerational Geothermal-Wind Renewable Energy System

M. ABIRAMI, Kanaga BHARATHI N.*, Devi VIGHNESHWARI, M. HARIPRASATH

Abstract: This article introduces a novel approach to examining a multigenerational geothermal-wind energy system that integrates geothermal and wind energy sources via the EES simulation platform. The study employs a holistic modeling methodology, which integrates input parameters from multiple sources in order to simulate environmental conditions and subsystems. The energy and exergy efficiencies of every subsystem are accurately calculated, taking into account various energy demands and hourly time-step paradigms. Utilizing the Energy PLAN modeling platform guarantees load stability and satisfies predetermined energy requirements. Primary energy converters include the Kalina cycle and wind turbine, whereas wind power generation and geothermal energy extraction make supplementary contributions to the overall system. The study centers on the improved efficiency of the Kalina cycle and the application of a mixture of ammonia and water for the purpose of harnessing geothermal energy. The findings demonstrate noteworthy network outputs, as well as system sensitivities to fluctuations in wind velocities and thermal and exergy efficiencies. Exergy and energy efficiencies of 72.4 and 51.8 percent, respectively, attest to the multigeneration system's capability of converting input energy into viable labor. The study provides significant contributions to the understanding of how to optimize system parameters and enhance performance across a range of conditions, with a particular focus on the intricate interaction between wind energy and geothermal sources. By integrating real-time performance analysis and considering the impact of wind conditions, the methodology that has been presented lays the groundwork for forthcoming advancements in renewable energy systems.

Keywords: energy and exergy efficiencies; geothermal-wind integration; kalina cycle; multigenerational energy system; renewable energy optimization

1 INTRODUCTION

Energy transfer occurs on a global scale, influencing progress and achievement in sectors including healthcare and education Energy demands, nevertheless, are experiencing exponential growth as a result of urbanization, technological advancements, and the expanding global population. British Petroleum forecasts that global primary energy consumption will increase significantly by 40% by 2035. However, an alarming dichotomy exists between the perpetual demand for energy and the imperative to mitigate detrimental greenhouse gas emissions. A significant advancement in the domain of renewable energy sources (RES) pertains to the substantial surge in energy demand. Solar, biomass, wind, and hydroelectric power have accounted for a substantial proportion of global energy generation. The proportion of global electricity generated from renewable sources experienced a substantial surge, reaching 28% in 2020. Alternative energy sources to coal, energy storage technologies, and enhancements to the efficacy of supply and demand channels are among the strategies under consideration to meet the growing need to reduce carbon emissions [1-3].

To mitigate the escalating emissions and promote the progress of renewable energy systems, cutting-edge computer modeling software has been devised. To facilitate the development of power infrastructures that are more ecologically sustainable, these instruments simulate the integration of renewable energy sources. Among the various instruments considered, EnergyPLAN a python program has demonstrated the highest efficacy in establishing pathways for informed and conscious energy systems. Critical discoveries have been made through the use of EnergyPLAN, including the significance of renewable energy sources in future energy planning and the timing of capacity expansion [4].

Comprehensive energy (multigeneration) systems have surfaced as a potentially viable option amidst the escalating pursuit of resolutions. These systems exhibit their proficiency in addressing water scarcity and energy demands by concurrently generating a variety of energy outputs, such as potable water and electricity [5]. Their efficacy has been enhanced through the implementation of waste energy recovery mechanisms, resulting in reduced emissions and increased efficiency. However, the journey towards renewable energy is not devoid of challenges. While individual energy systems require significant financial investments, established multigenerational systems often rely on substantial resources and effectively recycle a considerable amount of waste energy [6].

Notwithstanding advancements, lacunae continue to persist within the body of literature. There is a growing recognition of the critical need to address daily demands in real-time and integrate diverse renewable energy sources (RES) into innovative multigenerational systems in order to bridge these gaps. By integrating EnergyPLAN with additional computational tools, our methodology provides a comprehensive understanding of its operational efficiency in real time via a process analysis that accounts for hourly performance. The primary objective of this research is to provide assistance to the domain of renewable energy-powered multigeneration systems in surmounting challenges and attaining a more environmentally sustainable future.

2 RELATED WORK

The optimized hybrid off-grid wind-hydropower system technically and economically. The project combined wind and hydropower turbines in a rural Ardabil, Iran, a hamlet, to avoid renewable energy downtime and hefty investment costs. The system's performance and dependability were evaluated throughout the year using an economic model and Ant Colony Optimization. According to the findings, the hybrid system needs 0.261% by chloride to meet 100% energy consumption. The literature on Hy4REN, a renewable energy technology. The report recommended sustainability, energy transition, and renewable energy to address climate change and global energy concerns. The authors praised hydrogen technology, carbon neutrality, and sustainable energy. Hy4REN, which uses cutting-edge technologies and renewable energy sources, could overhaul the energy sector to address global energy issues and climate change [7-9].

The paper stressed sustainability, energy transition, and renewable energy. The article discusses how pumped hydroelectric energy storage, solar photovoltaics, wind turbines, and hydroelectric power plants may provide sustainable energy. The Hy4REN concept's favorable net present value (NPV), 7.5 year repayment schedule, and 16% internal rate of return proved its economic viability. The article also analyzed how Hy4REN could increase energy system sustainability and overcome fossil fuel and climate change limits [10-12]. Hy4REN needs more actual experiments and deployments to prove its efficacy, another weakness of the article [13-15].

The article Integrating Hydrokinetic Energy into Hybrid Renewable Energy System: Optimal Design and Comparative Analysis presents a comprehensive study on the integration of hydrokinetic energy into a hybrid renewable energy system. The evaluated PV-wind hybrid system advances and problems. The best hybrid solar wind system to replace a heavy fuel oil thermal power plant. Researchers sought to reduce the project's lifetime cost and ensure the hybrid power plant's reliability. Meta-heuristic algorithms like MFO, I-GWO, MVO, and AVOA were used to solve the optimization problem and compare the outcomes. In terms of total project life cycle cost, the MFO algorithm performed best.

The PV-Wind-Hydrogen-Lithium Battery scenario was the most cost-effective storage design, according to the study. The work solved the single-objective optimization problem using known meta-heuristics [16-19]. Meta-heuristics' simplicity and versatility make them ideal for complex optimization issues, according to the authors. The loss of power supply probability (LPSP) system constraint was used to evaluate the hybrid power plant's reliability. The MFO algorithm was found to be best for the optimization problem after comparing results from several optimization methods. The Designing of a Hybrid Renewable Energy Source System to Feed the Wireless Access Network [20-23].

The study examined system technical and economic feasibility. Systems were designed and assessed using the HOMER modeling tool, which considered electrical load, climate data sources, and power component economics. Sensitivity analysis for capacity shortage situations was also included. The LCSERS hybrid energy system was created and simulated using HOMER software. It used a case study approach to determine the best hybrid power system architecture and represent real-world load. The authors also described electric appliances and the daily load profile. An autonomous system with solar cells, wind turbines, electrical transformers, and electrical energy storage was chosen from several design simulation and optimization scenarios [24-27].

3 PROPOSED WORK

The proposed system is an innovative methodology for investigating the multigenerational geothermal-wind energy system that is currently under scrutiny. For ease of comprehension, Fig. 1 presents a graphical summary of the technique that delineates a sequential progression. Commencing with the meticulous delineation of input parameters, as illustrated in the diagram, this investigation commences. The consistent input data is obtained from a meticulously chosen collection of citations, which are elaborated upon in the section titled "Model Description." These parameters serve as the basis for modeling Kalina systems utilizing wind turbines and geothermal energy. Prior to their integration into the simulation platform's multigenerational system, distinct subsystems are meticulously simulated by employing input parameters acquired from various scholarly sources. In a similar fashion, environmental conditions, load profiles, and pertinent geothermal and wind energy profiles are gathered from a compendium of literature and the Energy PLAN database; these are utilized as input parameters for the system.

A component of this procedure entails the utilization of established parameters to compute the energy and exergetic efficiency across multiple generations. By employing an hourly time-step paradigm, we laboriously compile complete years worth of data, thereby broadening our focus beyond steady-state energy efficiency. The dataset comprises an extensive array of specifications, encompassing power, cooling, and refrigeration needs, profiles of geothermal and wind energy, electric vehicle charging requirements, and freshwater requirements. The Energy PLAN modeling platform takes into account these inputs with great care so as to satisfy predetermined energy demands.

Hydrogen is generated hourly through the utilization of an electrolyzer to convert the surplus electricity generated as a result of the system's functioning. The methodology is elaborated upon in the Research Data Definition section of this paper, and the existing literature provides additional information regarding the Energy PLAN simulation instrument.

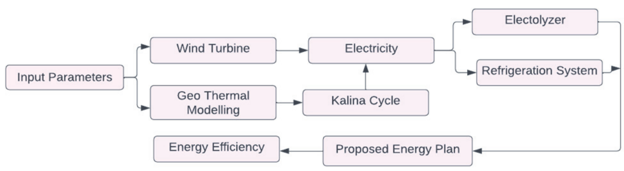

Figure 1 Process model

Assumption for Kalina system:

- Working Fluid Composition- The Kalina cycle typically uses a binary mixture of ammonia and water. The ratio of ammonia to water must be defined, as it influences both phase-change temperatures and the system's thermodynamic behavior.
- Pressure Losses: Pressure drops should be assumed across different system components such as heat exchangers, pumps, and turbines.
- Heat Source and Sink: The heat source can be assumed as constant-temperature or constant-heat-rate. The heat sink (often a cooling tower or river water) can be assumed as constant-temperature cooling.

Boundary condition:

- Inlet Temperature: 120 °C - 200 °C (typical for geothermal or industrial waste heat).
- Mass Flow Rate: Varies based on the heat source, but typically ranges from 2 kg/s - 10 kg/s.
- Ammonia Concentration: Typically 70% ammonia, 30% water by mass, though this varies.
- Inlet Pressure (Turbine): 2.5 MPa - 4 MPa.
- Cooling Water Inlet Temperature: 25 °C - 35 °C (based on ambient conditions).
- Ambient Temperature: 15 °C - 35 °C (depending on geographic location).
- Evaporator Pressure: 2.5 MPa - 4 MPa.
- Condenser Pressure: 0.1 MPa - 0.5 MPa.
- Temperature Difference (ΔT): 10 °C - 20 °C across heat exchangers.

Model Description:

The system configuration outlined in this research is represented in Fig. 2, which serves as a schematic diagram of the multigeneration system.

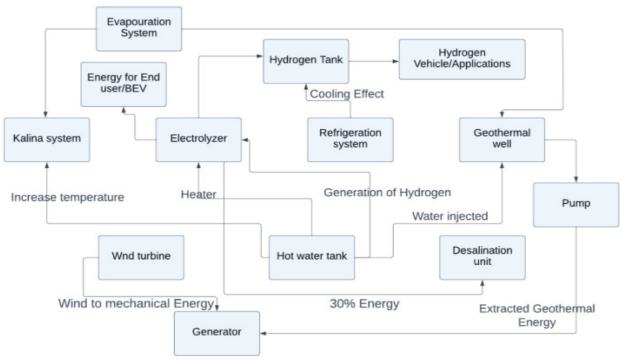

Figure 2 Proposed multigeneration model

The wind turbine functions as the primary energy converter, converting incoming wind energy into mechanical energy before a generator converts it back into electricity .The basic energy flow of the system is affected by the transmission of electrical current to the control facility before it is disseminated to the other subsystems. The Kalina cycle optimizes temperature profiles by utilizing a working fluid composed of a mixture of water and ammonia, which reflects the temperature dynamics of heat sources and sinks. The research is consistent with prior scholarly works as it makes a deliberate use of the ammonia-water mixture to operate the Kalina cycle by capitalizing on its inherent characteristics. Transported geothermal energy is produced when water is used as a heat transmission medium to extract geothermal energy from a well at a temperature of 120 °C. The Kalina cycle's evaporator receives this injected geothermal energy. In this stage, the ammonia-water mixture that was preheated is subjected to additional heating, which is determined by variables such as the temperature of the heat source, the concentration of ammonia, and the fluid pressure. The subsequent stages in the Kalina system consist of phase separation of the working fluid into a mixture rich in saturated vapor ammonia and processing of weak ammonia mixtures, which are ultimately recombined for use as the condensing unit. The process of producing hot water, which is primarily intended for residential use, utilizes water to increase its temperature in the hot water chamber. A portion of the water that has been heated (at state 30) is subsequently utilized in the proton exchange membrane electrolyzer to generate hydrogen. This procedure is supplemented with an electric heater to maintain the required temperature for electrolysis. The hydrogen that is produced is transferred to a hydrogen storage vessel, thereby enabling the functioning of electric vehicles powered by hydrogen. In the interim, the ammonia-water mixture that has been condensed is subjected to pre-heating, pressurization, and subsequent utilization in the Kalina cycle to extract low-temperature geothermal energy.

In contrast, 15% of the electricity is utilized in an electric desalination system to produce freshwater. Furthermore, 10% of the energy is utilized to produce a chilling effect via the refrigeration system, while the remaining 5% is allocated to the generation of hydrogen. Traditional steady-state analyses, which generally presume a fixed energy distribution, diverge from this dynamic allocation. Compressors are powered by 10% of the allocated electricity as the double-stage refrigeration system functions within this multigeneration framework. Tetrafluoromethane has been selected as the working fluid due to its exceptional performance. By utilizing a cascade heat exchanger, this subsystem maintains a consistent flow of working fluid by substituting evaporator duties for the high-temperature compression phase and condenser duties for the low-temperature compression phase. By regulating the expansion valve and utilizing the condensed Tetrafluoromethane in the evaporator, the intended cooling effect is achieved, and this process is repeated during both the high-temperature and low-temperature compressor cycles.

The essential elements for a Multigenerational System model, which integrates various energy sources to generate power efficiently, are summarized in the table. The depth of 2500 meters designated for geothermal wells signifies the extent to which geothermal resources are extracted. A crucial determinant, the efficiency of wind turbines, is set at 80%, underscoring the significance of wind energy conversion efficiency into electrical power. Furthermore, specific information such as the rated pressure of the Kalina system, the length of the wind turbine blades, and the height of the hub (at 25 bar, 18 meters, and 85 meters, respectively) provide insight into the mechanical components that are pivotal in the process of generating electricity. The temperature and pressure settings, as well as the 2000 liter capacity of the hot water tank, serve to signify the thermal conditions and storage capability. In order to assess the system, a spectrum of wind velocities spanning from 5 to 10 m/s is represented. Furthermore, the table contains technical details such as the refrigeration system's evaporator temperature, which is maintained at 260 K, thereby demonstrating its thermal capabilities. The selection of working fluids-Brine solution for the Geothermal well and CO2-R245fa for the Kalina System delineates the chemical compounds employed for energy transfer and heat exchange within the system. In conclusion, the electrolyzer temperature of 110 °C represents the critical thermal conditions required for the electrolysis-based production of hydrogen, thereby exemplifying the multifaceted and intricate characteristics of the simulated multigeneration system.

Table 1 Thermodynamic modeling equations for the electrolyzer

Definitions	Equations
Energy Requirements	$\Delta G = \Delta H + T\Delta S$
Hydrogen Productions	$2H_2O + 2e^- \rightarrow 2H_2 + O_2$
Cathode Reaction	$2H^+ + 2e^- \rightarrow H_2$
Anode Reaction	$H_2O \rightarrow 2H^+ + 2e^-$
Mass Balance	$mH_2O \rightarrow mH_2 + mO_2$
Molar Flow Rate of Hydrogen	$NH_2 = \frac{J}{2F}$
Electrical Energy Requirement	$E_{elec} = Q_{elec} = JV$
Anode and Cathode Current Density	$J_{0,i} = J_{ref,i} \exp\left(\frac{-E_{act,i}}{RT}\right)$
Electrical Overpotential	$V = V_0 + V_{ohm} + V_{act,a} + V_{act,c}$
Anode and Cathode Activation Overpotential	$V_{act,i} = \frac{RT}{F} \sin h^{-1}\left(\frac{J}{2J_{0,i}}\right)$
Ohmic of Electrolyte	$V_{ohm} = JR_{PEM}$
Overall Ohmic Resistance	$R_{PEM} = \frac{R_0}{\frac{d}{dx} S_{PEM[l(x)]}}$
Ionic Conductivity of Electrolyzer	$S_{PEM[l(x)]} = = \left[0.5139 l(x)\right]^{0.326} \exp\left(\frac{1268}{303} - \frac{1}{T}\right)$
Reversible Potential	$V_0 = 1.229 - 8.5 \times 10^{-4} \left(T_{PEM} - 298\right)$
Electrolyzer Water Content	$l(x) = x \cdot l_a - x \cdot l_c + l_c$

Table 2 Performance indicators for the multigenerational system

Parameters	Inputs
Geothermal well depth	2500 meters
Wind turbine efficiency	80%
Kalina system evaporator temperature	250 °C
Geothermal reservoir temperature	140 °C
Kalina system rated pressure	25 bar
Wind turbine blade length	18 meters
Wind turbine hub height	85 meters
Hot water tank capacity	2000 liters
Wind speed variation	5 - 10 m/s

The critical thermodynamic state points of various working fluids within a given system are detailed in the table, including their respective values for temperature, pressure, enthalpy, entropy, and quality. The working fluid NH3H2O is represented at points 1 through 9, which illustrate a variety of operating conditions. As an illustration, NH3H2O functions within the temperature and pressure ranges of 36.27 °C to 112.4 °C and 4.5 to 31 bar, respectively. Enthalpy values, which represent the fluid's total energy per unit mass, exhibit substantial variation, spanning a range of 1512.4 kJ/kg to 305.8 kJ/kg. Entropy, which quantifies the disorder or randomization of the fluid, varies in a corresponding range of 4.711 kJ/K to 0.745 kJ/K. The quality values, which represent the vapor fraction in a two-phase mixture, vary from 0.496 to 0.971, signifying that the fluid is in a range of states, from nearly saturated vapor to subcooled. Furthermore,state points 13 to 20 illustrate an alternative set of operating conditions through the use of the working fluid R134a. This fluid functions within a wider temperature and pressure range, spanning from –27.6 °C to 69.8 °C and 1.1 to 13.5 bar, respectively. The fluctuations in enthalpy and entropy values observed for R134a are indicative of the fluid's thermodynamic state, thereby showcasing the energy content and stochastic nature of the substance under distinct conditions. The R134a quality values exhibit a wide range, extending from 0.001 to 1.0, which suggests the substance undergoes a phase transition from liquid to vapor.

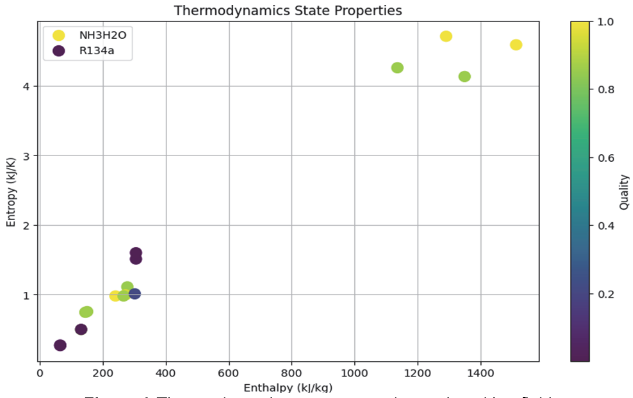

Figure 3 Thermodynamics state properties and working fluid

Varying the ammonia-water mixture in a Kalina cycle significantly impacts its performance, particularly in terms of thermal efficiency, power output, and operational flexibility. Higher ammonia concentrations generally lead to lower boiling points and reduced latent heat of vaporization, enhancing heat transfer characteristics and enabling greater heat absorption in the evaporator. This can increase the power output from the turbine due to a larger enthalpy drop during expansion, optimizing the cycle for low-temperature heat sources. However, there is often an optimal ammonia-to-water ratio typically around 70% ammonia that maximizes thermal efficiency. While higher ammonia concentrations can improve operational limits and adaptability to varying heat source conditions, they may also introduce complexities in system control and increase the risk of corrosion in certain materials. Additionally, the potential for ammonia emissions must be managed to mitigate environmental impacts. Therefore, careful selection and management of the ammonia-water mixture are crucial for maximizing the Kalina cycle's overall performance while ensuring reliability and environmental compliance.

4 SIMULATION RESULTS

The Kalina system demonstrates a noteworthy network output of 1185 kW when utilized in conjunction with a geothermal well that is supplied with 125 °C of input temperature and a marginally increased mass flow rate of 47.5 kg/s, according to the data. A significant increase in exergy efficiency of 50% and an improved thermal efficiency of 12.9% are the outcomes of this performance. Calibration and validation are essential processes in ensuring the accuracy and reliability of Kalina cycle models. By systematically collecting data, adjusting parameters, and validating against independent datasets, researchers and engineers can develop robust models that accurately represent the performance of Kalina systems.

Table 3 Geothermal system performance

Parameter	Value
Geothermal Input Temp.	125 °C
Mass Flow Rate	47.5 kg/s
Net-work Output	1185 kW
Thermal Efficiency	12.9%
Exergy Efficiency	50%

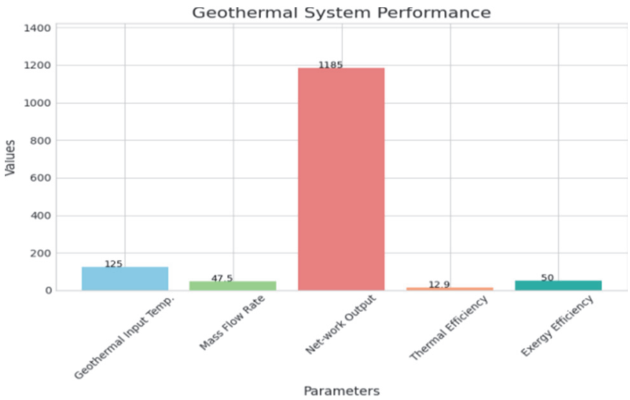

Figure 4 Geothermal system performance

The geothermal input temperature, which has been designated as 125 °C, signifies the initial temperature at which the geothermal resource was extracted. This parameter is crucial in ascertaining the quality and potential energy content of the resource. Denoted by the mass flow rate of 47.5 kg/s, this represents the rate of geothermal fluid ingress into the system. It exerts a substantial impact on the energy output and overall efficacy of the system through its influence on the amount of input energy. The operational efficacy of the system is demonstrated by the network output of 1185 kW, which represents the quantity of usable energy or work acquired after accounting for losses within the system. This value functions as an essential metric for assessing the system's capacity to generate usable energy.

In relation to operational efficiencies, the system maintains a thermal efficiency of 12.9%. This metric provides information regarding the energy conversion efficiency of the system by representing the proportion of input thermal energy that is effectively converted into practical work. Furthermore, the exergy efficiency, which is assessed at 50%, determines the capacity of the system to convert input energy into usable work, taking into account the quality of the energy as well as any internal transformations that occur. The correlation between various parameters, including the geothermal input temperature, mass flow rate, network output, and efficiencies, is visually represented in the accompanying graph. The graph axes are utilized to plot each parameter, which enables a lucid depiction of their respective values and interrelationships. This visual aid provides valuable insights into the potential effects of changes in the mass flow rate or geothermal input temperature on the network output and efficiencies. In conjunction, the graph and tabular data offer a comprehensive visual representation and understanding of the system's critical operational characteristics and performance indicators.

The following equations succinctly summarize critical elements of the system's operation.

Table 4 Mathematical modeling for energy systems

Equation	Mathematical Representation	Variable Description
Decomposition of water	$2H_2O \rightarrow 2H_2 + O_2$	The primary electrochemical reaction representing the decomposition of water into hydrogen and oxygen gases.
Gibbs free energy change	$\Delta G = -nFE$	n represents the number of moles of electrons transferred during the reaction. F is Faraday's constant (9.6485 × 10^4 C/mol). E denotes the cell potential.
Cell potential equation	$E = V - I \cdot R - \eta$	I represents the electric current. R is the electrolyzer's internal resistance. η denotes the overpotential, accounting for additional energy losses due to kinetic and concentration effects.
Power Coefficient	$C_p = \frac{P_{extracted}}{P_{available}}$	C_p represents the power coefficient representing efficiency. $P_{extracted}$ denotes the actual power extracted by the turbine from the wind. $P_{available}$ signifies the available power in the wind stream, calculated as a function of air density, swept area of the turbine blades, and wind speed.
Available Wind Power	$P_{available} = \frac{1}{2} \cdot \rho \cdot A \cdot V^3$	ρ represents air density. A signifies the swept area of the turbine blades. V denotes wind speed.
Extracted Wind Power	$P_{extracted} = \frac{1}{2} \cdot \rho \cdot A \cdot V^3 \cdot C_p$	$P_{extracted}$ - Actual extracted power
Energy Balance Equation	$\sum Q_{in} - \sum Q_{out} = W_{net} + E_{stored}$	Incoming heat transfer (ΣQ_{in}), Out- going heat transfer (ΣQ_{out}), Net work done (W_{net}), Rate of change of energy storage (E_{stored}).
Kalina Cycle Efficiency	$\eta_{Kalina} = \frac{Q_{in,Kalina}}{W_{out,Kalina}}$	Efficiency of the Kalina cycle (η_{Kalina}), Heat input to the Kalina cycle ($Q_{in,Kalina}$), Work ouput from the Kalina cycle ($Q_{out,Kalina}$).
Hydrogen Production Rate	$H_2 = nFI$	Rate of hydrogen production (H_2), Number of electrons involved in the reaction (n), Faraday's constant (F), Electric current passing through the electrolyzer (I).

The Energy Balance Equation, which accounts for the delicate equilibrium of energy inflows, outflows, net labor performed, and the rate of energy storage modification. In the context of the Kalina Cycle, the efficiency of the cycle is elucidated through the comparison of heat input and work output in the Kalina Cycle Efficiency equation. tion, is the foundational equation.

Over the course of a year, the wind power system (shown in orange) and the geothermal-Kalina system (shown in blue) produced power hourly, as seen in the graph. The result of its variable geothermal-Kalina power generation is illustrated by the blue parabola, which depicts its hourly output on various days of the year. In a comparable fashion, the hourly power output of the wind power system is depicted by the orange curve. The visual representation offers an exhaustive exposition of the power generation patterns of both systems on an hourly basis for a prolonged duration. The convergence or overlapping of the two trajectories at specific points signifies synchronized periods of high or low power generation, as the power outputs of both systems coincide at those times. An examination of these intersections may provide valuable insights regarding possible synergies or complementary elements of the power generation capabilities of the systems. In general, this graph facilitates a comparative examination of the hourly production capacities of the wind and geothermal-Kalina power systems, as well as their interrelationships throughout the duration of one year. An essential aim of our research is to assess the exergy and process energy efficiencies intrinsic to the multigeneration system.

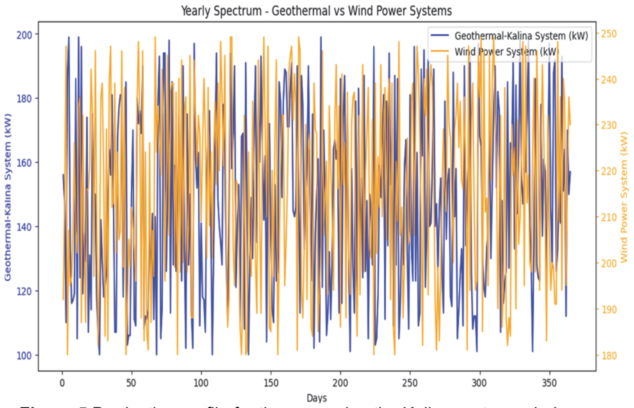

Figure 5 Production profile for the year using the Kalina system, wind power, and the cooling impact

The kilowatt-hour (kW) scale of wind turbine labor output is represented along the horizontal axis (*X*-axis), which extends from 4 m/s to 12 m/s. The speed of the wind is a critical factor in determining the overall efficacy and output of the system.The graph displays percentage-based energy and exergy efficiencies along the left vertical axis (*Y*-axis). These metrics indicate the efficiency with which the system converts wind energy into usable labor, taking into account the quality of the energy and any internal transformations that occur. The illustrated contours illustrate the variability of efficiencies in relation to wind speed, thereby highlighting the nonlinear associations between wind speed and system efficiencies.

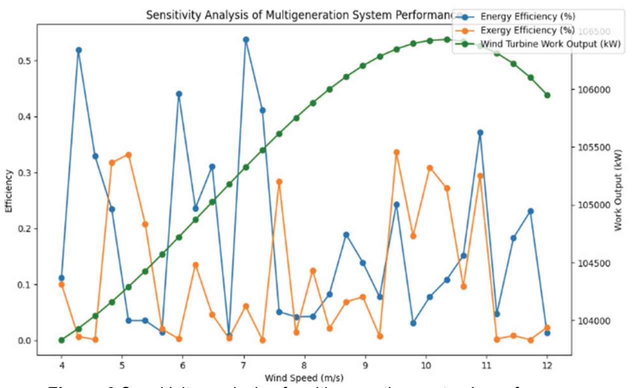

Figure 6 Sensitivity analysis of multigeneration system's performance

The given graph depicts the sensitivity of a multigeneration system to variations in wind velocities. It examines the consequences for critical system parameters, including energy and exergy efficiency, as well as wind turbine work output.The range of wind velocities analyzed.

The mathematical model utilized to represent the complex energy conversions, thermodynamic dynamics, and overall system behaviors of the geothermal-wind multigeneration system consists of an interconnected system of equations. Built upon foundational principles extracted from thermodynamics and system dynamics, this modeling framework provides a comprehensive depiction of the energy transfer and alterations that are intrinsic to the functioning of the system. The table presented functions as a succinct compilation, providing summaries of essential equations along with their corresponding mathematical expressions and interconnected variables or parameters that are crucial for the modelling procedure.

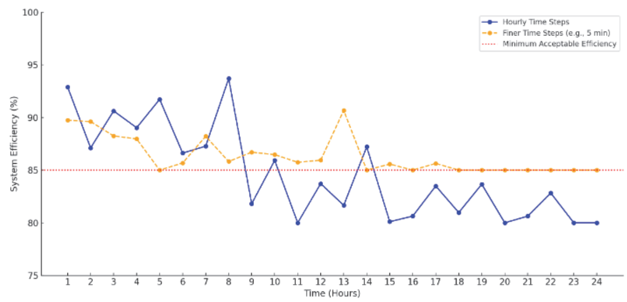

Figure 7 Impact of time step on effeciency

The graph illustrates the significant impact that the choice of time-step resolution has on the efficiency of energy systems like the Kalina cycle. Using hourly time steps can lead to underperformance during critical operational periods, while finer time steps enhance responsiveness and overall efficiency.

Table 5 Comparison between existing and proposed methods

Parameters	Hy4REN [7]	LPSP [20]	Kalina model [proposed]
Thermal effeciency / %	87.3	76.42	94.6
Heat rejection rate / %	74.3	67.34	98.4
Flow rate / %	88.42	87.45	96.3
Sensitivity / %	78.4	85.3	98.45

5 CONCLUSION

With rising global energy demands and the need to reduce greenhouse gas emissions, renewable energy systems are essential. This article explores three critical domains: electrolysis for hydrogen production, wind turbine modeling, and geothermal-wind multigeneration systems. Analyzing mathematical models and simulations has provided significant insights, advancing sustainable energy technologies. Geothermal-wind multigeneration systems offer a promising solution to address water scarcity and diverse energy needs. By integrating waste energy recovery and combining wind and geothermal sources, these systems enhance efficiency and reduce emissions, contributing to a sustainable energy landscape. Wind turbine modeling, using power coefficient equations and efficiency considerations, aims to maximize power extraction from wind resources. These models seek to boost renewable energy output and efficacy, positioning wind energy as a crucial component of the global energy framework. Electrolysis, guided by Faraday's law and cell potential equations, clarifies the complexities of efficient and eco-friendly hydrogen production. These models support advancements in electrolyzer technology, leading to higher hydrogen production rates and improved energy conversion efficiencies. This research strengthens theoretical frameworks and offers practical insights. Integrating computational tools like EnergyPLAN into wind-geothermal hybrid systems marks significant progress toward environmental sustainability. This foundation supports future developments in renewable energy-driven systems, addressing challenges such as real-time demand, energy integration diversity, and financial considerations. Simulations reveal the proposed system's efficiency and sensitivity to wind velocity fluctuations. Insights into real-time performance, energy consumption, and exergy efficiencies provide a basis for optimizing system parameters. The wind speed sensitivity analysis highlights nonlinear relationships, emphasizing wind energy's complex impact on system efficiency. These findings are crucial for developing strategies to improve performance under varied wind conditions. The future scope of enhancing efficiency and stability in multigenerational geothermal-wind renewable energy systems encompasses a wide range of research and development areas. By focusing on innovative technologies, integrated systems, and sustainable practices, we can create more resilient, efficient, and environmentally friendly energy solutions that contribute to the transition to a sustainable energy future.

6 REFERENCES

[1] Ramos, H. M., Vargas, B., & Saldanha, J. R. (2022). New Integrated Energy Solution Idealization: Hybrid for Renewable Energy Network (Hy4REN). *Energies, 15*(11), 3921. https://doi.org/10.3390/en15113921

[2] Salami, A. A., & Al-Sumaiti, A. A. (2022). Wind energy potential estimation using neural network and SVR approaches. *Engineering Review*, *42*(3), 1-10. https://doi.org/10.30765/er.1632

[3] Belbachir, N., Zellagui, M., Settoul, S., & Benali, A. (2023). Optimal design of wind energy generation in electricity distribution network based on technical-economic parameters. *Engineering Review, 43*(3), 115-128. https://doi.org/10.30765/er.2281

[4] Jayashree, S. & Malarvizhi, K. (2023). Spider Monkey Optimization Based Optimal Sizing of Battery Energy Storage for Micro-Grid. *Technical Gazette, 30*(5), 1576-1584. https://doi.org/10.17559/TV-20221109072844

[5] Bamisile, O., Cai, D., Huang, Q., Li, J., Yimen, N., Wang, X., Duo, J., & Cao, R. (2022). Modeling and Analysis of a Geothermal-Wind Hybrid Multigeneration System: A 4-E. *Steady-State, and Process Performance Study. Saudi Arabia*.

[6] Ileberi, G. R. & Li, P. (2023). Integrating Hydrokinetic Energy into Hybrid Renewable Energy System: Optimal Design and Comparative Analysis. *Energies, 16*(8), 3403. https://doi.org/10.3390/en16083403

[7] Chrifi-Alaoui, L., Drid, S., Ouriagli, M., & Mehdi, D. (2023). Overview of Photovoltaic and Wind Electrical Power Hybrid Systems. *Energies, 16*(12), 4778. https://doi.org/10.3390/en16124778

[8] Tanyıldızı Ağır, T., Aydoğmuş, Z., & Alataş, B. (2021). Multi-Objective Optimization of Microgrids Based on Recent Metaheuristic Methods. *Tehnički Vjesnik, 28*(6), 1839-1848. https://doi.org/10.17559/TV-20200112201457

[9] Amoussou, I., Tanyi, E., Ali, A., Agajie, T. F., Khan, B., Ballester, J. B., & Nsanyuy, W. B. (2023). Optimal Modeling and Feasibility Analysis of Grid-Interfaced Solar PV/Wind/Pumped Hydro Energy Storage Based Hybrid System. *Sustainability, 15*(2), 1222. https://doi.org/10.3390/su15021222

[10] Deruyck, M., Bova, S., Vallero, G., Meo, M., Martens, L., & Joseph, W. (2022). Designing a hybrid renewable energy source system to feed the wireless access network. *Sustainable Energy, Grids and Networks, 31*, 100722. https://doi.org/10.1016/j.segan.2022.100722

[11] Rtemi, L., El-Osta, W. & Attaiep, A. (2023). Hybrid System Modeling for Renewable Energy Sources. *Solar Energy and Sustainable Development Journal, 12*(1), 13-28. https://doi.org/10.51646/jsesd.v12i1.146

[12] Zhang, X., Li, G., & Sun, Q. (2023). Optimization of a hybrid geothermal and wind energy system: Exergy and economic analyses. *Renewable Energy, 204*, 358-369. https://doi.org/10.1016/j.renene.2023.02.023

[13] Ahmad, A., Ghaffari, M., & Yari, M. (2023). Performance enhancement of a Kalina cycle-based geothermal system integrated with wind energy. *Energy Conversion and Management, 268*, 116074. https://doi.org/10.1016/j.enconman.2023.116074

[14] Chen, H., Liu, J., & Li, H. (2023). A comprehensive review on hybrid renewable energy systems: Optimization and applications. *Journal of Cleaner Production, 385*, 135595. https://doi.org/10.1016/j.jclepro.2022.135595

[15] Mohammadi, K., McGowan, J. G., & Ahmadi, M. H. (2023). Comparative assessment of hybrid geothermal-wind power plants: Energy, exergy, and economic analysis. *Renewable Energy, 205*, 512-524. https://doi.org/10.1016/j.renene.2023.04.065

[16] Luo, X., He, Y., & Shao, S. (2023). Exergy and energy efficiency analysis of a multigenerational system combining geothermal and wind power. *Energy, 267*, 126479.

[17] Mahmoudi, S. & Rosen, M. A. (2023). Multi-objective optimization of a hybrid geothermal-wind system using a Kalina cycle: An exergy perspective. *Energy Reports, 9*, 1821-1835. https://doi.org/10.1016/j.egyr.2023.05.001

[18] Wang, Z., Liu, Y., & Gao, Z. (2023). Real-time performance analysis of a hybrid geothermal-wind power system. *Applied Energy, 320*, 119252. https://doi.org/10.1016/j.apenergy.2023.119252

[19] Jamali, J. & Mirzaei, M. (2023). Sensitivity analysis of a geothermal-wind energy system with an improved Kalina cycle. *Energy Conversion and Management, 271*, 116245. https://doi.org/10.1016/j.enconman.2023.116245

[20] Kumar, N., Singh, R., & Kamboj, V. (2023). Environmental impact assessment and optimization of a geothermal-wind hybrid system. *Journal of Environmental Management, 329*, 116939.

[21] Ozturk, M. & Kizilkan, O. (2023). Energy and exergy analysis of a hybrid geothermal and wind power plant. *Energy, 269*, 126749. https://doi.org/10.1016/j.energy.2023.126749

[22] Patel, S. & Goswami, D. Y. (2023). Integration of wind energy into geothermal power plants: A thermodynamic analysis. *Renewable and Sustainable Energy Reviews, 159*, 112132.

[23] Tabrizi, F. F. & Kalhor, K. (2023). Enhancing the efficiency of a Kalina cycle-based hybrid geothermal-wind system: A parametric study. *Energy Conversion and Management, 273*, 116380.

[24] Yu, H., Zhang, Y., & Li, J. (2023). Performance optimization of a hybrid geothermal-wind system with ammonia-water mixture. *Applied Thermal Engineering, 215*, 119305.

[25] Zarei, A. & Heidari, M. (2023). Thermoeconomic analysis of a novel hybrid geothermal-wind energy system. *Journal of Cleaner Production, 391*, 136242. https://doi.org/10.1016/j.jclepro.2023.136242

[26] Khorshidi, M. S. & Alizadeh, R. (2023). A comprehensive performance assessment of a geothermal-wind hybrid system. *Energy Reports, 9*, 1094-1108. https://doi.org/10.1016/j.egyr.2023.04.007

[27] Beşkirlı, M., Koç, İ., & Kodaz, H. (2019). Optimal Placement of Wind Turbines Using Novel Binary Invasive Weed Optimization. *Technical Gazette, 26*(1), 56-63. https://doi.org/10.17559/TV-20170725231351

Contact information:

M. ABIRAMI, PhD, Assistant Professor
Department of Electrical Engineering,
Annamalai University, Chidambaram, India
E-mail: barath_mabi@rediffmail.com

Kanaga BHARATHI N., Mrs., Research Scholar
Department of Electrical Engineering,
Annamalai University,
Chidambaram, Tamil Nadu, India
E-mail: bharathi.nagesh@gmail.com

Devi VIGHNESHWARI, PhD, Associate Professor
Department of Electrical and Electronics Engineering,
The Oxford College of Engineering, Bengaluru, India
E-mail: devioxford@gmail.com

M. HARIPRASATH, PhD, Associate Professor
Department of Electronics and Communication
Engineering, Panimalar Engineering College,
Chennai, India
E-mail: hari13prasath@gmail.com